REPORT DOCUMENTATION PAGE

AFRL-SR-BL-TR-02-

0078

1. AGENCY USE ONLY (Leave blank)	2. REPORT DATE	3. REPORT TYPE
	December 13, 2001	February 19[illegible]

4. TITLE AND SUBTITLE
Rare Earth Nanophosphors

5. FUNDING NUMBERS
F49620-99-1-0158

6. AUTHOR(S)
Stephen C. Rand

7. PERFORMING ORGANIZATION NAME(S) AND ADDRESS(ES)
University of Michigan
EECS Department
1301 Beal Avenue, 1112 EECS Bldg.
Ann Arbor, MI 48109-2122

8. PERFORMING ORGANIZATION REPORT NUMBER

9. SPONSORING / MONITORING AGENCY NAMES(S) AND ADDRESS(ES)
AFOSR/NE
110 Duncan Avenue, Sutie B115
Bolling AFB, DC 20332-8080

10. SPONSORING / MONITORING AGENCY REPORT NUMBER

11. SUPLEMENTARY NOTES
The views, opinions and/or findings contained in this report are those of the author(s) and should not be construed as an official Department of the Army position, policy or decision, unless so designated by other documentation.

12a. DISTRIBUTION / AVAILABILITY STATEMENT
Approved for public release; distribution unlimited.

12b. DISTRIBUTION CODE

13. ABSTRACT (Maximum 200 words)

This project initiated a systematic investigation of doped nanodielectrics as optical materials in which *strong scattering conditions* offer prospects of new, low-voltage phosphors and high brightness surface lighting in the ultraviolet and visible spectral regions. The research effort succeeded in demonstrating not only new phosphors, but electrically-pumped stimulated emission in random powders and advances in the synthesis of dielectric nanophosphors suitable for bright source applications of many kinds, including flat panel display technologies, target identification, communication and authentication. As outlined in this report, results achieved during the project period considerable exceeded scientific objectives in both the quantum electronic and materials areas, by achieving the first continuous-wave laser operation at ultraviolet and visible wavelengths in several electrically-pumped powders. We also obtained the first direct evidence of stationary light in a structureless medium, that is, light of zero velocity created by a new approach to strong Anderson localization.

14. SUBJECT TERMS

15. NUMBER IF PAGES
16

16. PRICE CODE

17. SECURITY CLASSIFICATION OR REPORT	18. SECURITY CLASSIFICATION OF THIS PAGE	19. SECURITY CLASSIFICATION OF ABSTRACT	20. LIMITATION OF ABSTRACT
UNCLASSIFIED	**UNCLASSIFIED**	**UNCLASSIFIED**	**UL**

"Rare Earth Nanophosphors"

Final Technical Report

Research Grant AFOSR 49620-99-1-0158
(Project Period 2/1/99-11/30/01)

Principal Investigator: Professor S.C. Rand

AIR FORCE OFFICE OF SCIENTIFIC RESEARCH

Program Manager
Dr. Howard Schlossberg

November 30, 2001

FINAL TECHNICAL REPORT

"Rare Earth Nanophosphors"
(2/1/99 - 11/30/01)

1. Project Description

1.1. Introduction

This project initiated a systematic investigation of doped nanodielectrics as optical materials in which *strong scattering conditions* offer prospects of new, low-voltage phosphors and high brightness surface lighting in the ultraviolet and visible spectral regions. The research effort succeeded in demonstrating not only new phosphors, but electrically-pumped stimulated emission in random powders and advances in the synthesis of dielectric nanophosphors suitable for bright source applications of many kinds, including flat panel display technologies, target identification, communication and authentication. As outlined in this report, results achieved during the project period considerably exceeded scientific objectives in both the quantum electronic and materials areas, by achieving the first continuous-wave laser operation at ultraviolet and visible wavelengths in several electrically-pumped powders. We also obtained the first direct evidence for stationary light in a structureless medium, that is, light of zero velocity created by a new approach to strong Anderson localization.

2. Objectives

The initial, main objectives of this project were to:

- Demonstrate a simple, electrically-pumped, omni-directional, UV/VIS light source and display technology utilizing nanophophors dispersed in a conducting medium
- Demonstrate unexpectedly intense emission in RE-doped nanoparticles on new intra-configurational transitions (RE^{3+}=Ce, Pr, Nd, Tm, Yb)

Secondary objectives were intended both for basic characterization and to provide insight into optical properties of doped nanopowders, to open the door to future work on quantum size effects:

- Measure fluorescence decay times of intra- and inter-configurational transitions of RE dopants versus dielectric particle size to determine if quantum size effects manifest themselves on single-photon radiative transitions, causing enhanced emission
- Search for systematic variations in multi-photon upconversion emission intensities and linewidths in RE-doped nanoparticles versus particle size and concentration - evidence of quantum size effects on multi-photon radiative transitions

3. Experimental Result Summary

3.1. Electron Excitation - Numerical Computations

Electrical generation of spontaneous emission in phosphors requires charge carriers to penetrate the medium and to excite luminescent centers within it. To achieve stimulated

emission, one would think that like all other materials phosphors would have to furnish sufficient gain over the distance that light could propagate without severe attenuation to achieve a gain length product of unity. Since the gains in rare earth materials are less than 10^3 cm^{-1} and attenuation lengths are less than a wavelength in our nanopowders, this would seem to be an impossible task in rare-earth-doped dielectric nanophosphors. However, much to our surprise, we have discovered that continuous-wave laser action is possible in these materials through multiple-scattering interference effects that cause a phenomenon known as strong Anderson localization of light. To provide a basis for understanding our experiments, it was therefore important from the outset of this project to calculate the average distance traveled by energetic electrons into the interior of our phosphors. For this purpose the collisional trajectories of many incident electrons accelerated by a known voltage into the chosen host had to be calculated and averaged.

Monte Carlo simulations of electron trajectories in alumina were run on a variety of workstations for this purpose. Average penetration depths of electrons in alumina were calculated using a particle scattering algorithm [1]. Our routine was capable of computing classical trajectories for electrons of kilovolt initial energies in any material of known density and scattering cross section. The residual electron energy that signaled the end of each calculation was 50 eV, which is exceptionally low for numerical codes of this type, but was essential for accurate modeling of our problem. Mott scattering cross sections were used for the Al and O constituents of our powders because of the low energy range of our experiments. The results are shown in Fig. 1 and have interesting implications when compared with the transport distance for light measured by coherent back-scattering (See Sec. 4.2). Calculations of the penetration of electrons and their comparison with measurements of optical transport distances furnishes an initial basis for understanding the balance of excitation rate, excitation depth and the extraction of optical output from highly attenuating nanopowders. This point is discussed further in Section 4.

3.2. Materials Preparation

As planned in our original proposal, we prepared metallorganic precursors for use in synthesizing Nd and Gd-doped nanopowders by a simple flame spray pyrolysis technique. Initial synthesis focused on the growth of δ-phase Al_2O_3, and production of this phase-pure ceramic material was confirmed upon simple flame spray pyrolysis of the precursors using our patented technique [2]. The nanopowders generated by this method were found to be unagglomerated, faceted, single crystals of mean diameter <40 nm. This morphology is evident in Figure 2(a). Initially, a small amount (~5%) of over-sized particles (diameter ~1 micron) was discovered by Coulter particle size analysis. However, nozzle replacement and modifications in the growth conditions sufficed to eliminate this problem. This permitted us to maintain the concentration of unwanted particle size below 0.1%. Good agreement was then found with average particle size estimates based on SSAs and equivalent sphere models (Micromeritics ASAP 2000), and the measured size distribution was accurately log-normal (Figure 2(b)).

Amongst the available rare earth ions, Nd^{3+} and Gd^{3+} are both potential candidates for stimulated emission in the ultraviolet when electrical pumping is used. This is due to an

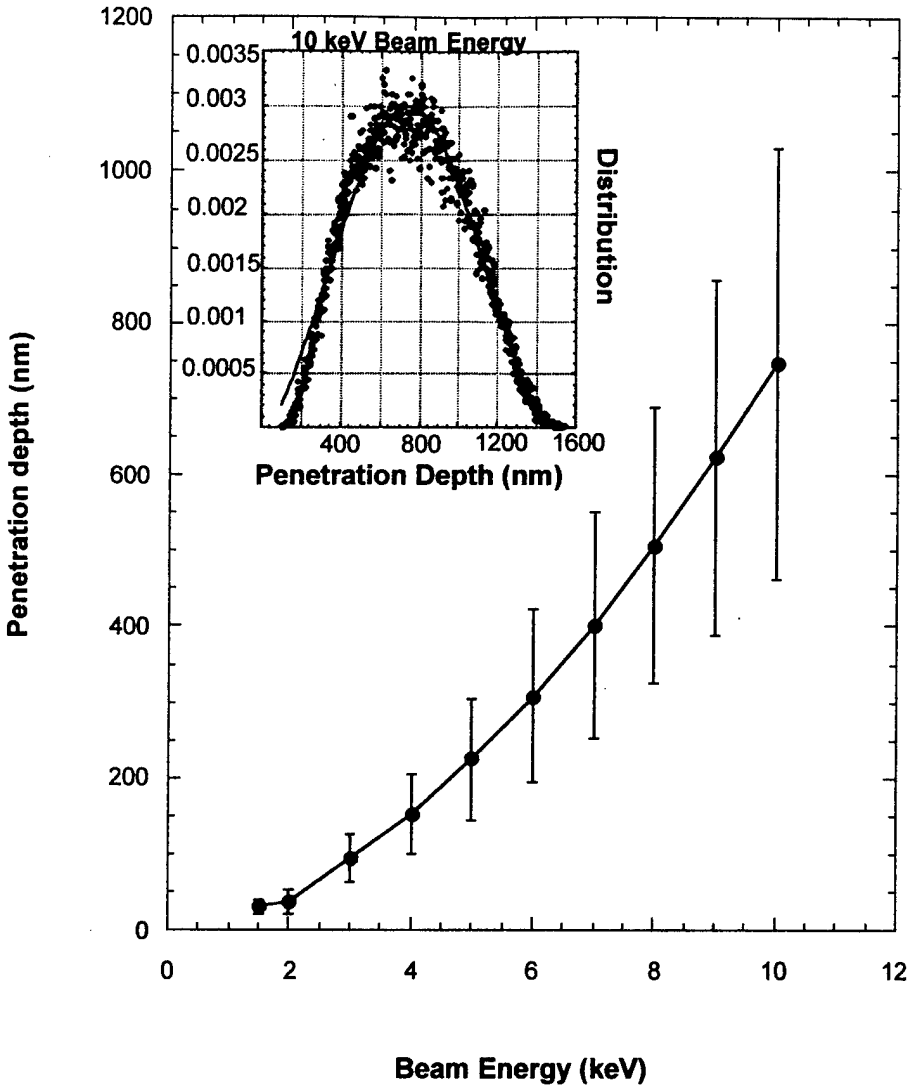

Figure 1. Simulation of electron penetration depths in alumina, based on the CASINO algorithm [1]. Each point is the result of many trajectory calculations for a given electron energy. These calculations generate a curve similar to the inset, which illustrates the distribution obtained in this way for 10 keV.

accommodating electronic structure, which allows both for efficient transfer of electrical excitation from the oxide host to the $4f^n$ configuration of the rare earth dopants, and short wavelength emission from high energy states of the impurities. No difficulties or changes in morphology were encountered while incorporating up to 1 mole% rare earth in alumina. Similarly, no difficulties were encountered in the preparation of metallorganic precursors utilizing alternative rare earth dopants, as described next.

While the preferred habit for pyrolytic synthesis in alumina was shown to be the δ-phase, precursors for other phases such as β", which includes Na and Li constituents, were also prepared. Attempts were then made to stabilize the direct production of these other phases during pyrolysis. However these efforts were not successful. The β"-phase could be formed only upon subsequent annealing at 1600 degrees. Undesirable agglomeration that normally occurs during such post-growth procedures, so no annealing or calcining was acceptable in alumina samples that were subsequently used for stimulated emission experiments. Because of the versatility of our pyrolytic technique, synthesis of additional powders with dopants other than Nd and Gd was possible during the project period. Powders of Pr^{3+}: Al_2O_3, Eu^{3+}:Al_2O_3, Tm^{3+}:Al_2O_3, Tb^{3+}:Al_2O_3, Ho^{3+}:Al_2O_3, and Er^{3+}:Al_2O_3 were all prepared successfully with particle sizes in the <40 nm range. A concentration series was prepared in Er^{3+}:Al_2O_3 powder.

Finally, samples of co-doped Er,Yb:Y_2O_3 were made using mixed precursors in the same approach. No annealing was required to form phase-pure samples of Yttria. This finding is important for future work, since Yttria is a more common host oxide for rare earth ions than alumina. Its successful synthesis by our pyrolysis technique opens the door to more straightforward comparisons of optical properties dielectric nanophosphors with those of conventional phosphors.

3.3. Optical Experiments

3.3.1. *Emission Spectroscopy*

Cathodoluminescent (CL) spectra were recorded with a 1-meter grating spectrometer by mounting powder samples in a small UHV chamber equipped with an electron gun and UV- transmitting optical ports. At room temperature, extensive sets of spectra were recorded at different electron currents and different voltages in samples of Nd^{3+}:δ-Al_2O_3 and Gd^{3+}:δ-Al_2O_3. In the former samples, numerous emission lines from Nd appeared throughout the UV and visible spectral regions. These lines underwent remarkable changes as the current was increased (in the range 0-100 μA), and this excitation dependence is discussed later in the context of stimulated emission. Similar experiments on the Gd-doped powders were also performed.

Experiments with Pr^{3+}:δ-Al_2O_3, Tm^{3+}:δ-Al_2O_3 and co-doped Yb^{3+},Er^{3+}:δ-Al_2O_3 nanopowders were also undertaken. The Pr sample showed relatively uncomplicated cathodoluminescence spectra, dominated by a single red transition. This made it convenient to study sample emission reliably as a function of voltage at a single wavelength, so numerous recordings were made of output intensity in the red versus excitation current at voltages in the 1-10 keV range.

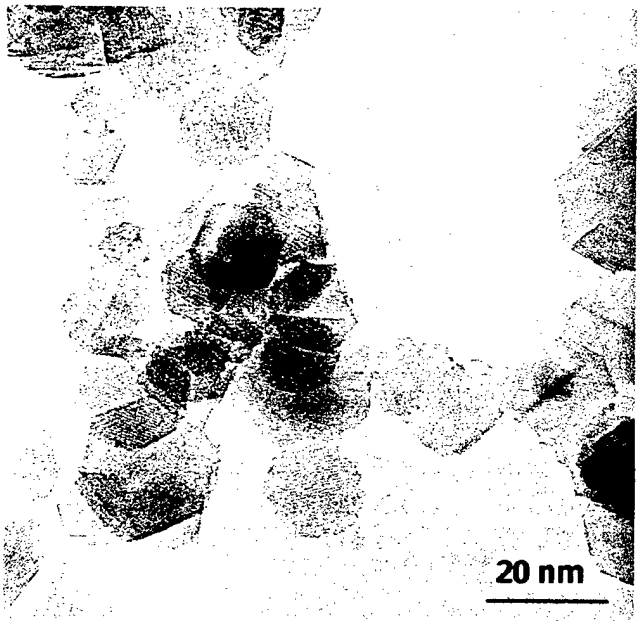

Figure 2(a). Transmission electron micrograph of δ-Al_2O_3 nanoparticles. Note the faceted edges and the unaggregated state of particles in the sample.

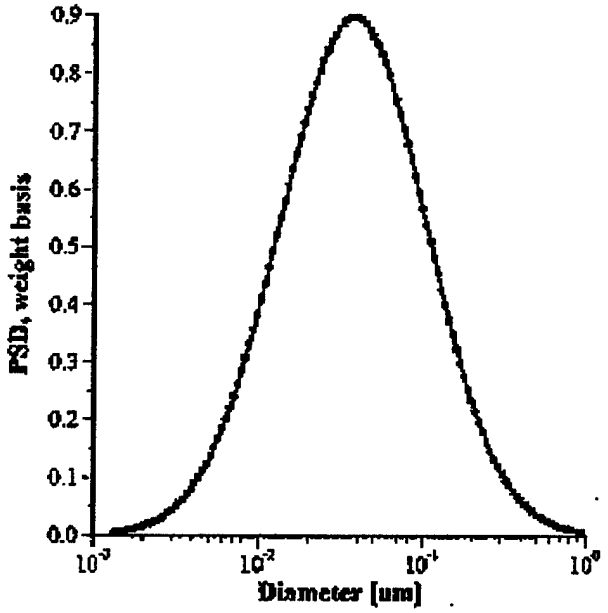

Figure 2(b). Size distribution of undoped Ceria nanoparticles synthesized by flame spray pyrolysis.

Thulium has absorptive transitions in the 800 nm region that overlap the output range of Ti:sapphire lasers. Hence with available laboratory sources we were able to scan through the near IR spectral region (770-850 nm) and to observe three main upconversion lines from Tm^{3+} in preliminary spectroscopic surveys. Upconversion emission results from multi-photon dynamics within individual rare earth ions or from multi-atom dynamics occurring within coupled ion clusters. Since both types of upconversion mechanism are potentially sensitive to changes in the non-radiative decay within nanosystems, measurements of this kind will be useful in future research to identify size-related changes in the optical properties of nanopowders, by comparing excitation and lifetime dynamics with upconversion in single crystals, with which we have extensive experience. In the co-doped Yb^{3+},Er^{3+}:δ-Al_2O_3 nanopowders, emission spectra and emitted intensity on selected lines were measured as a function of incident intensity at 940 nm. At this wavelength Yb absorbs strongly on a vibronic transition and subsequent energy transfer to Er leads to the emission of upconverted, visible light. In the nanopowder sample however, unexpected behavior was observed, as described in the next section.

Turn-around time was a significant problem throughout most of this project due to limitations of our original vaccum chamber (Fig.3). Each time sample exchange was needed, the UHV chamber had to be cycled up to atmospheric pressure. This caused long delays and occasionally introduced leaks into parts of the system that were not even disassembled, eventually necessitating an extension of the project. Additionally, samples could not be manipulated inside the original chamber and no surface diagnostics were available. Had we been able to correct this undesirable situation earlier many more results could have been obtained. Equipment funding from a block educational grant in 2001 finally permitted us to assemble a new UHV chamber with improved sample transport, manipulation, and surface characterization (Fig. 3). This facility is already greatly accelerating the pace of advances in follow-on experimentation.

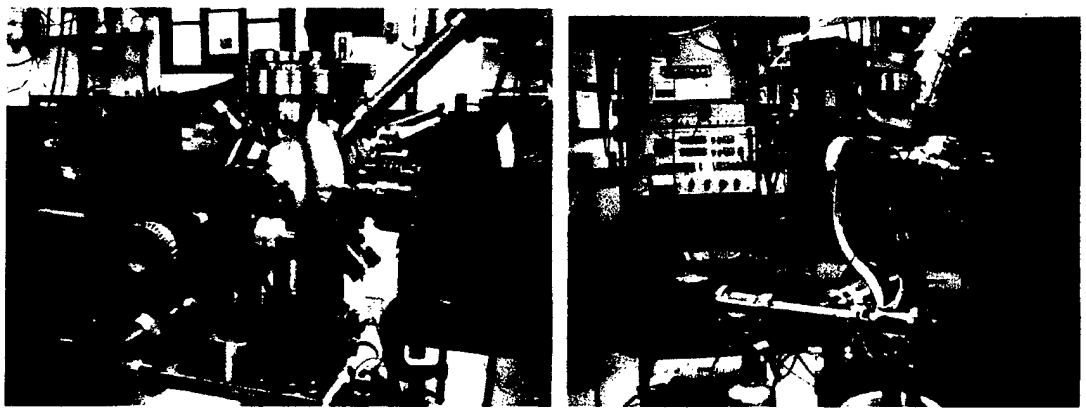

Figure 3. New (left) and old (right) ultrahigh vacuum chambers for cathodoluminescence spectroscopy of rare earth nanophosphors.

3.3.2. *Coherent Back-Scattering*

In order to characterize optical propagation in our samples, measurements of the transport mean free path l* were made using three separate approaches to coherent back-scattering (CBS). Apparatus that was used in preliminary experiments was rebuilt in the first three months of the project to improve angular resolution and introduce computer control. The rebuilt setup used a rotating detector geometry and a miniature turning mirror. Subsequently, two other CBS setups were assembled - one based on a rotating detector geometry with a beam splitter to permit back-scattered intensity to be measured at vanishingly small angles, and one based on a rotating sample geometry. All three setups provided independent experimental determinations of l* from observations of the back-scattering cone. Together with the planned introduction of an electronically-variable polarization rotator, these improvements will permit automated (tensorial) evaluation of transport with all possible combinations of incident and exiting polarizations. During the project period, manual polarization selections were sufficient to investigate wave transport in both transverse dimensions on the surface of our powders.

4. Results and Discussion

4.1. Stimulated Emission

In Fig.4, complete optical emission spectra are shown that were recorded at different current levels in a sample of Nd^{3+}:δ-Al_2O_3. Numerous emission lines assignable to Nd^{3+} are evident throughout the UV and visible spectral regions, and they undergo remarkable changes as the current is increased. By examining the spectroscopic assignments of lines in the neighborhood of 300-370 nm, it was possible to conclude that emission from the $^2F_{5/2}$ state was quenched on all transitions to lower states save one, the $^2F_{5/2}$ - $^4F_{3/2}$ transition, at current levels >40 μA. An example of a quenched feature originating from $^2F_{5/2}$ is the line at 32,500 cm^{-1}. This line is prominent at 10 μA and absent at 40 μA. The disappearance of emission lines which have the same upper state ($^2F_{5/2}$) as a transition which becomes prominent as excitation increases is direct evidence of stimulated emission in the upper ($^2F_{5/2}$) state. The increase in the emission rate of one channel that overwhelms the constant rate in other channels is uniquely explained by the onset of stimulated emission.

Identical quenching behavior was observed for another state in the Nd samples. Emission on the $^2P_{1/2}$ -$^4I_{11/2}$ transition also grew in intensity above a sharp "threshold" value of electron current, as shown in Fig. 5(a). At 10 μA, all other emission lines originating from the $^2P_{1/2}$ state disappeared. An example of a quenched line is the feature at 23,000 cm^{-1}. Because the output curves have different slopes above and below the threshold point, and are linear above and below this point, they provide direct evidence of electrically-pumped, continuous-wave laser action in Nd powder on blue and ultraviolet

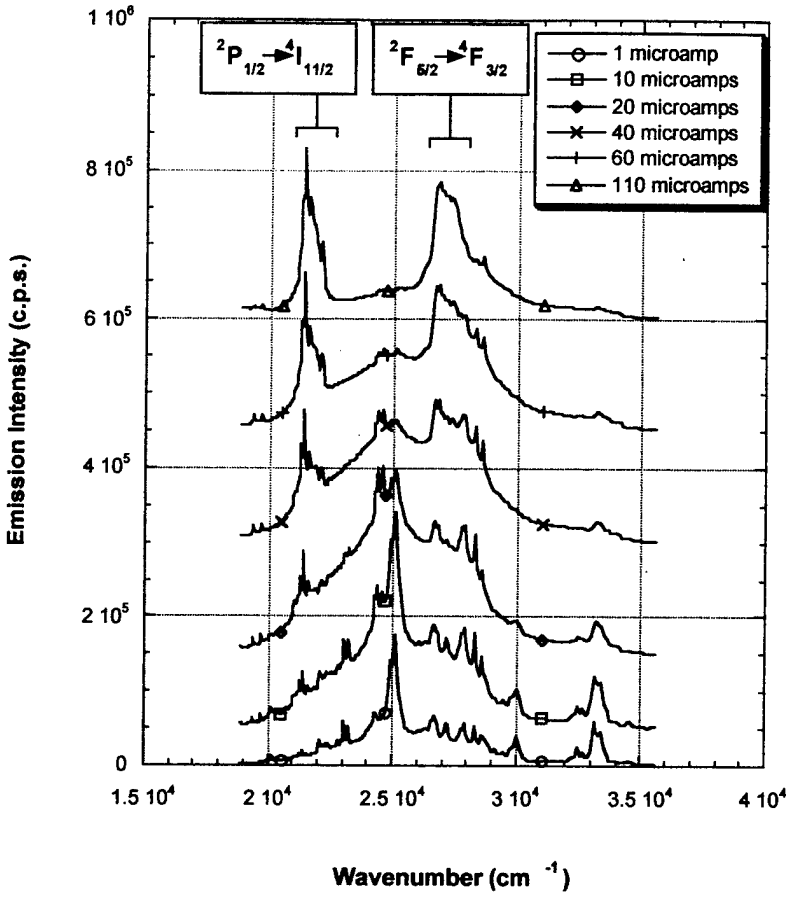

Figure 4. Cathodoluminescence spectra of Nd^{3+}:δ-Al_2O_3 excited at various current levels with 7 keV electrons in ultrahigh vacuum.

transitions indicated, at room temperature. Similar experiments in Ce^{3+}:δ-Al_2O_3 also revealed a threshold and ultraviolet laser action at 363 nm (Fig 5(b)).

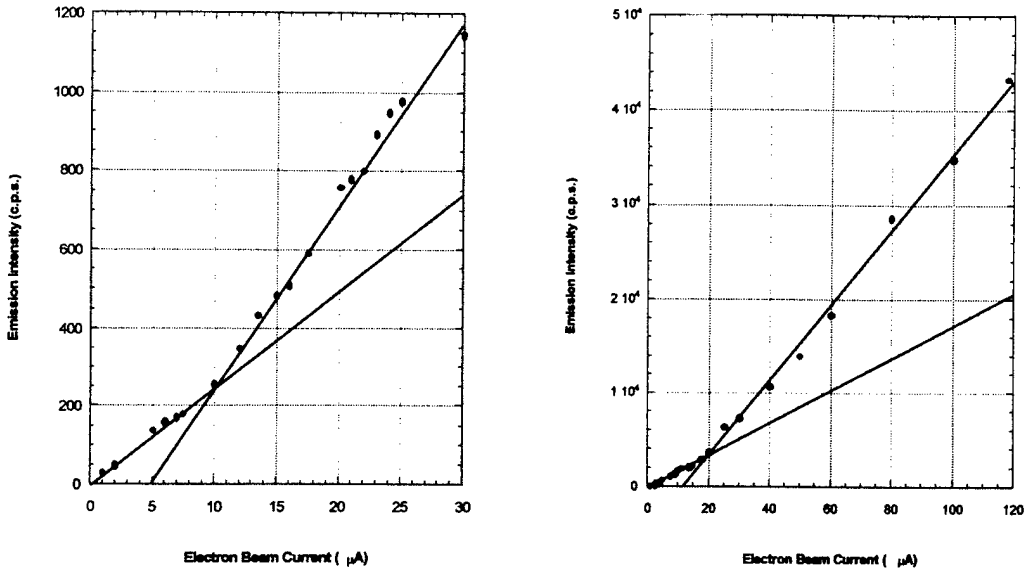

(a) (b)

Figure 5. Cathodoluminescent intensity versus current in a sample of (a) Nd^{3+}:δ-Al_2O_3, and (b) Ce^{3+}:δ-Al_2O_3, each showing two linear output regimes separated by abrupt transitions at currents of 10 μA and 20 μA respectively.

Experiments on Gd-doped powders were unsuccessful. Although the $^6P_{3/2}$ - $^8S_{7/2}$, $^6P_{5/2}$ - $^8S_{7/2}$, and $^6P_{7/2}$ - $^8S_{7/2}$ ultraviolet emission lines were readily observed (Fig.6), their intensity was found to saturate so quickly at low currents that the shape of the output curve could not be reliably deduced. Consequently, equipment limitations at low current levels made it very difficult to provide any convincing evidence of population inversion in these samples. This tendency of Gd emission to saturate quickly is undoubtedly due to the extended lifetimes of the ^6P excited states of Gd, which have large energy gaps with respect to the ground state and are spin-forbidden to decay radiatively to ground. It therefore remains to be seen whether Gd samples can exhibit continuous stimulated emission at room temperature.

Similar measurements in Pr^{3+}:δ-Al_2O_3 samples revealed striking emission thresholds and a strong voltage-dependence of the observed threshold currents (Fig. 7). A significant finding was that the thresholds observed in Pr emission were lowest and most abrupt at voltages near 4-5 keV, whereas at lower voltages the thresholds were higher. This was in semi-quantitative agreement with our computations of electron penetration. At this voltage electrons penetrate a distance into the medium that is approximately equal to l^*. It seems reasonable to infer that matching the depth of the excitation volume to the transport length minimizes radiative losses on the scale length of the optical feedback, while still providing for the escape of some light from the interior to serve as the signal.

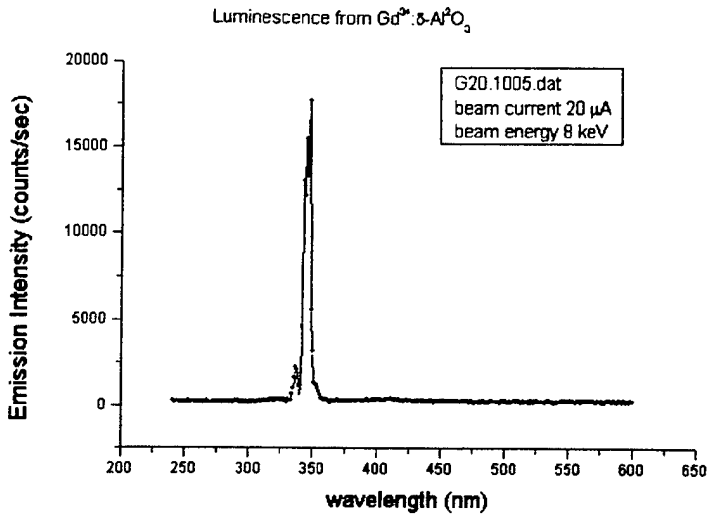

Figure 6. Ultraviolet luminescence of Gd^{3+}:δ-Al_2O_3 nanopowder at room temperature, excited by an electron beam in ultra-high vacuum at a current of 20 μA and an accelerating voltage of 8 keV. Three transitions originating from the $^6P_{3/2}$, $^6P_{3/2}$, and $^6P_{3/2}$ excited states that terminate in the $^8S_{7/2}$ ground state of Gd are evident.

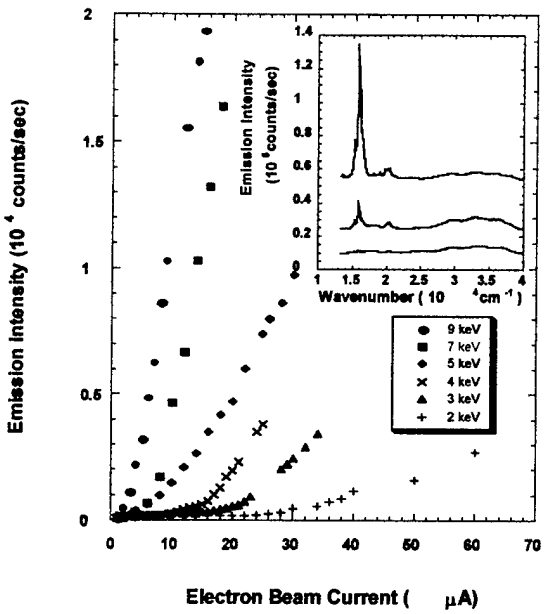

Figure 7. Emission intensity versus current at λ_{ex}=632.8 nm in Pr^{3+}:δ-Al_2O_3 nanoparticles and electron energy (1-10 keV). Inset: Emission spectra of Pr^{3+}:δ-Al_2O_3 illustrating growth of the red transition with increasing current at 7 keV.

In fact, the voltage provides a means of adjusting the output coupling of light from the interior of the powder by changing the depth at which most of the incident kinetic energy of the electrons is deposited.

4.2. Optical Transport

Our measurements by several independent CBS techniques provided self-consistent determinations of the optical transport mean free path l* in our samples. For example at 632.8 nm (the wavelength of the He-Ne laser) analysis of Pr^{3+}:δ-Al_2O_3 data in the inset of Fig. 8 and the lower trace both yield l*=311 nm. In the upper trace, data for a Ce^{3+}:δ-Al_2O_3 sample yield l*=114 nm.

Using laser light selected to overlap Ce, Nd and Pr emission wavelengths, determinations of l* were made at a number of optical wavelengths to investigate the spectral dependence of strong scattering in preliminary measurements. In samples showing stimulated emission thresholds, the value of l* at all test wavelengths was invariably found to be lower than λ/2. Such values are among the shortest transport lengths ever reported for lossless elastic scattering at optical frequencies. Results to date are shown in Fig. 9, and suggest that the interval over which our samples exhibit their unusual properties may extend throughout the visible and ultraviolet spectral regions.

5. Conclusions

During the grant period, observations of spectral quenching (Fig.4), and linear output above clearly-defined stimulated emission thresholds in Nd^{3+}, Ce^{3+} and Pr^{3+} nanophosphors (Figs. 5, 7) furnished compelling evidence of continuous-wave (cw) laser action at wavelengths in the ultraviolet, blue and red spectral regions. Conventional cavities support cw laser action only with high reflectivity mirrors. Hence one can infer from our observations that light experiences strong reflection in all directions within our samples. At the same time, CBS measurements directly confirm that light is severely attenuated in less than half a wavelength, in all directions with respect to the emitting ion. Given that absorption is negligible ($\lambda << l_\alpha$), these experimental results indicate that light generated within our powders acquires a spatial distribution that is exponentially small outside a volume on the order of a cubic wavelength containing the emitter. We conclude that this behavior indicates strong electromagnetic localization over a wide range of optical frequencies.

Simulations of electron penetration in alumina provided insight into the strong voltage dependence of stimulated emission thresholds. A physical picture emerged in which emission is stimulated coherently over distance scales on the order of tens of nanometers in our samples, but spatial randomization on the length scale of half a wavelength precludes directionality or mode selectivity. Back-scattered light (and laser output) appears to be virtually speckle-free, consistent with its sub-wavelength effective coherence length. Finally, all frequencies within the luminescent linewidth experience comparable gain and feedback independent of observation angle, just as expected for continuous, truly "random" laser action.

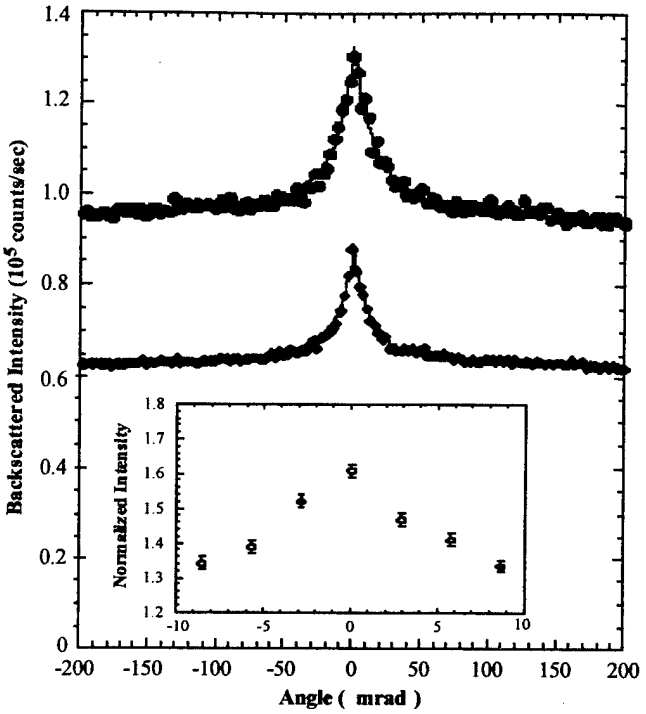

Figure 8. Experimental back-scattered intensity versus angle at λex=363.8 nm (upper trace) and λex=632.8 nm (lower trace), from Ce^{3+}:δ-Al_2O_3 and Pr^{3+}:δ-Al_2O_3 nanoparticles respectively (polarization ⊥ scan plane). Solid curves are best fits to standard CBS theory. Inset: Detail of the sharp, central cusp in Pr^{3+}:δ-Al_2O_3, showing normalized peak intensity of 1.61 after corrections for beamsplitter reflectivity.

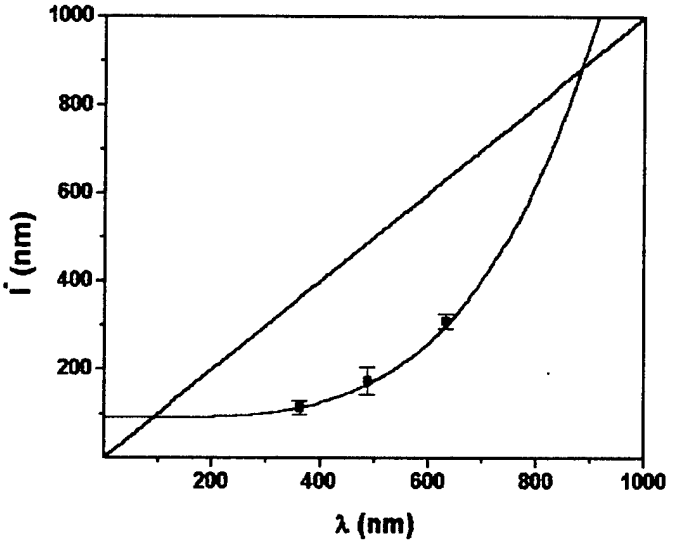

Figure 9. Experimental values of mean free transport distances l* for light in nanoalumina, derived from CBS observations. Polarization of the incident light was perpendicular to the scanning plane, making the data points upper limits on l* at the indicated wavelengths. The curve through the data is a simple fit to a Rayleigh scattering curve to provide a guide to the eye of the range over which l*<λ.

These results identify Nd^{3+}:δ-Al_2O_3 as a blue laser phosphor. Ce^{3+}:δ-Al_2O_3 is shown to be an ultraviolet laser phosphor and Pr^{3+}:δ-Al_2O_3 yields red laser emission as the result of electrical pumping. The brightness of existing phosphors in televisions, fluorescent lights, plasma and field emission displays is strictly limited by the spontaneous emission rate, but this limitation can be overcome with stimulated emission of the type that we have demonstrated here for the first time. The absence of speckle in laser phosphor emission could facilitate large-area, sub-micron optical lithography. As the result of this work it seems clear that doped, dielectric nanophosphors may provide a versatile family of emissive materials for novel light sources. Additionally our preliminary comparisons of nanopowder upconversion with the emission of identically-doped single crystals show striking differences that suggest quantum size effects may play an important role in non-radiative processes in rare earth nanopowders. Many fundamental advances can be expected to emerge from these findings.

Confinement of light within sub-wavelength regions may mediate new or enhanced nonlinear phenomena associated with ultraslow light, recurrent scattering and surface resonances. We have demonstrated omni-directional stimulated emission that is achieveable on new transitions, in new wavelength ranges, with excitation methods not previously feasible in dielectrics. For example, our results for both Nd^{3+} and Ce^{3+} are the first to demonstrate continuous laser action on blue and ultraviolet transitions of these ions respectively by any means. Studies of the pseudo bandgap predicted to accompany Anderson localization and the dependence of optical coherence on proximity to the localization "edge" should now be feasible in nanodielectrics. Research on these topics will complement existing knowledge from electron studies of wave transport in a wide variety of disordered systems.

References:

1. R. Gauvin, P. Hovington, D. Drouin, Scanning, 19, 1-14(1997); ibid, pp. 20-28; ibid, pp. 29-35.

2. A.C. Sutorik, S.S. Neo, T. Hinklin, R. Baranwal, D.R. Treadwell, R. Narayanan, and R.M. Laine, J. Am. Ceram. Soc. 81, 1477-1488 (1998); R.M. Laine, K. Waldner, C. Bickmore, D. Treadwell, U.S. Patent 5,614,596 (March 1997).

APPENDIX

PUBLISHED PAPERS, CONFERENCE PROCEEDINGS & PATENTS

B. Li, S.R. Redmond, S.C. Rand, T. Hinklin, and R.M. Laine, Direct Evidence for Stationary Light", Quantum Electronics & Laser Science Conference (QELS '02) (submitted).

B. Li, S.M. Redmond, and S.C. Rand, "Continuous-wave ultraviolet laser action and optical properties of pyrolyzed Nd:δ-alumina", Conference on Lasers & Electro-optics (CLEO '02) (submitted).

S.M. Redmond, B.R. Furman, and S.C. Rand, "White light generation and trapping in Yttria nanopowders", Quantum Electronics & Laser Science Conference (QELS '02) (submitted).

G. Williams, B. Bayram, S.C. Rand, T. Hinklin, and R.M. Laine, "Laser action in strongly scattering rare-earth-doped dielectric nanophosphors", *Phys. Rev. A* (accepted).

B. Li, G.R. Williams, S.C. Rand, T. Hinklin and R.M. Laine, Continuous-wave ultraviolet laser action in strongly scattering Nd-doped alumina", Optics Letters (accepted).

S.C. Rand (invited), "Localization and trapping-mediated phenomena in dense nanopowders", Opt. Soc. Am. Annual Meeting, Long Beach, California, October 14-18(2001).

"Chromatic Switching and optical hysteresis in strongly scattering rare earth nanophosphors", Opt. Soc. Am. Annual Meeting, Long Beach, California, October 14-18(2001).

S.C. Rand, "Strong localization of light and photonic atoms", *Can. J. Phys.* 78, 625(2000).

R.M. Laine, T. Hinklin, G. Williams, and S.C. Rand, "Low-cost nanopowders for phosphor and laser applications by flame spray pyrolysis", *Mat. Science Forum* 343-346, 500-510(2000).

S.B. Bayram, T. Jiang, S. Redmond, G. Williams, and S.C. Rand, "Wavelength Dependence of Optical Transport in Strongly Localizing Rare Earth Media", Qu. Elect. & Laser Science Conf. (QELS 2000), San Francisco, May 7-12, 2000, paper JMB7.

S.C. Rand, G. Williams, T. Hinklin, R.M. Laine, "Laser Phosphors", Fifth Int. Conf. on the Science and Technology of Display Phosphors, San Diego, Nov. 8-10(1999), paper 8.2.

G. Williams, S.C. Rand, T. Hinklin, and R.M. Laine, "Ultraviolet laser action in strongly scattering Ce:alumina nanopowders", Conf. on Lasers and Electro-optics (CLEO'99), Baltimore, Maryland, May 23-28, 1999, paper CTuG5.

S.C. Rand, G.R. Williams, T. Hinklin, and R.M. Laine, "Blue and infrared laser action in strongly scattering Nd:alumina nanopowders", Conf. on Lasers and Electro-optics (CLEO'99), Baltimore, Maryland, May 23-28, 1999, paper CThT8.

R.M. Laine, S.C. Rand, T. Hinklin, and G. Williams, "Ultrafine Powders as Lasing Media", U.S. and international patents pending.

B. Li, S.C. Rand, T. Hinklin and R.M. Laine, "Continuous-wave ultraviolet laser action and optical properties of pyrolyzed Nd:δ-alumina", Invention disclosure (University of Michigan, December, 2001).

S.M. Redmon, S.C. Rand, T. Hinklin, R.M. Laine, B.R. Furman, "Method to fabricate single-crystal tubes from ceramic nano-powders with a low power laser", Invention Disclosure (University of Michigan, December, 2001).

G.R. Williams, "Laser Phosphors", Ph. D. dissertation, University of Michigan, 1999.

Reprints & Preprints